Published May 4, 2015

Replication of *Plasmodium* in reticulocytes can occur without hemozoin formation, resulting in chloroquine resistance

Jing-wen Lin,[1,9] Roberta Spaccapelo,[4] Evelin Schwarzer,[5] Mohammed Sajid,[1] Takeshi Annoura,[1] Katrien Deroost,[6] Raimond B.G. Ravelli,[2] Elena Aime,[4] Barbara Capuccini,[4,9] Anna M. Mommaas-Kienhuis,[2] Tom O'Toole,[7] Frans Prins,[3] Blandine M.D. Franke-Fayard,[1] Jai Ramesar,[1] Séverine Chevalley-Maurel,[1] Hans Kroeze,[1] Abraham J. Koster,[2] Hans J. Tanke,[2] Andrea Crisanti,[4,8] Jean Langhorne,[9] Paolo Arese,[5] Philippe E. Van den Steen,[6] Chris J. Janse,[1] and Shahid M. Khan[1]

[1]Leiden Malaria Research Group, Department of Parasitology, [2]Department of Molecular Cell Biology, and [3]Department of Pathology, Leiden University Medical Centre, 2333 ZA Leiden, Netherlands
[4]Department of Experimental Medicine, University of Perugia, Piazzale Gambuli, 06132 Perugia, Italy
[5]Department of Oncology, University of Torino, 10124 Torino, Italy
[6]Laboratory of Immunobiology, Rega Institute for Medical Research, KU Leuven - University of Leuven, 3000 Leuven, Belgium
[7]Department of Molecular Cell Biology and Immunology, Vrije University Medical Center, 1007 MB Amsterdam, Netherlands
[8]Department of Biological Sciences, Imperial College London, South Kensington Campus, SAF, London SW7 2AZ, England, UK
[9]Division of Parasitology, MRC National Institute for Medical Research, London NW7 1AA, England, UK

Most studies on malaria-parasite digestion of hemoglobin (Hb) have been performed using *P. falciparum* maintained in mature erythrocytes, in vitro. In this study, we examine *Plasmodium* Hb degradation in vivo in mice, using the parasite *P. berghei*, and show that it is possible to create mutant parasites lacking enzymes involved in the initial steps of Hb proteolysis. These mutants only complete development in reticulocytes and mature into both schizonts and gametocytes. Hb degradation is severely impaired and large amounts of undigested Hb remains in the reticulocyte cytoplasm and in vesicles in the parasite. The mutants produce little or no hemozoin (Hz), the detoxification by-product of Hb degradation. Further, they are resistant to chloroquine, an antimalarial drug that interferes with Hz formation, but their sensitivity to artesunate, also thought to be dependent on Hb degradation, is retained. Survival in reticulocytes with reduced or absent Hb digestion may imply a novel mechanism of drug resistance. These findings have implications for drug development against human-malaria parasites, such as *P. vivax* and *P. ovale*, which develop inside reticulocytes.

CORRESPONDENCE
Shahid M. Khan:
s.m.khan@lumc.nl

Abbreviations used: AS, artesunate; BP, berghepain; CQ, chloroquine; DV, digestive vacuole; FP, falcipain; Hb, hemoglobin; Hz, hemozoin; iRBC, infected red blood cell; PM, plasmepsin; RBC, red blood cell; RLI, relative light intensity; SD, sulfadiazine; Sz, schizont; Tz, trophozoites.

Clinical symptoms of malaria are associated with *Plasmodium* infection of RBCs. Human *Plasmodium falciparum* parasites catabolize more than half of the hemoglobin (Hb) in the RBCs (Goldberg, 2005). The amino acids derived from Hb proteolysis are used for protein synthesis and energy metabolism. The proteolysis of Hb is accompanied by the release of free heme, which is cytotoxic for the parasite and is rapidly detoxified and converted into hemozoin (Hz). Therefore, both Hb degradation and heme detoxification are considered to be essential for *P. falciparum* survival (Goldberg, 2005). The digestion of Hb is a conserved and semiordered process, which principally occurs within the acidified digestive vacuole (DV). After the initial cleavage

T. Annoura's present address is Dept. of Tropical Medicine, The Jikei University School of Medicine, Tokyo 105-0003, Japan.
R.B.G. Ravelli's present address is Institute of Nanoscopy, Maastricht University, 6200 MD Maastricht, Netherlands.
J.-w. Lin and J. Langhorne's present address is The Francis Crick Institute, London NW7 1AA, England, UK.

© 2015 Lin et al. This article is distributed under the terms of an Attribution–Noncommercial–Share Alike–No Mirror Sites license for the first six months after the publication date (see http://www.rupress.org/terms). After six months it is available under a Creative Commons License (Attribution–Noncommercial–Share Alike 3.0 Unported license, as described at http://creativecommons.org/licenses/by-nc-sa/3.0/).

The Rockefeller University Press $30.00
J. Exp. Med. 2015 Vol. 212 No. 6 893–903
www.jem.org/cgi/doi/10.1084/jem.20141731

Supplemental Material can be found at:
http://jem.rupress.org/content/suppl/2015/04/30/jem.20141731.DC1.html

The Journal of Experimental Medicine

Downloaded from jem.rupress.org on June 23, 2015

Published May 4, 2015

by aspartic and papain-like cysteine endoproteases, Hb unfolds and becomes accessible to further proteolysis by downstream proteases. In the *P. falciparum* DV, there are four aspartic proteases (plasmepsins) and two papain-like cysteine proteases (falcipains) capable of hydrolyzing native Hb (Goldberg, 2005; Subramanian et al., 2009). Gene disruption studies of hemoglobinases demonstrated that *P. falciparum* has developed redundant and overlapping Hb degradation pathways, demonstrating the importance of Hb digestion for the parasite (Liu et al., 2006; Bonilla et al., 2007). However, Hb is a poor source of methionine, cysteine, glutamine, and glutamate; in addition, human Hb contains no isoleucine and *P. falciparum* blood-stage parasite growth is most effective in culture medium supplemented with these amino acids, especially isoleucine (Liu et al., 2006). These data indicate that *P. falciparum* parasites are not only dependent on Hb digestion, but also import exogenous amino acids (Liu et al., 2006; Elliott et al., 2008).

Most studies on Hb degradation have been performed using *P. falciparum* maintained with mature RBCs (normocytes) in vitro. It is unknown whether observations on *P. falciparum* Hb digestion made in vitro can be directly translated to parasites replicating in vivo or for parasites developing in reticulocytes such as the human parasite *P. vivax* and *P. ovale*. For example, mechanisms of resistance to some drugs that interfere with Hb digestion and heme detoxification (e.g., chloroquine) differ between *P. vivax* and *P. falciparum* (Baird, 2004; Baird et al., 2012) indicating that there may be differences in their Hb digestion pathways.

To obtain a better insight into Hb digestion in parasites developing in vivo we used a rodent malaria parasite, *P. berghei*, which preferentially invades reticulocytes. We show a high level of functional redundancy among the predicted hemoglobinases, as 6 of the 8 are dispensable in vivo. Unexpectedly, we were able to create parasite mutants lacking the enzymes known to initiate Hb digestion. These parasites were able to multiply in reticulocytes without Hz formation and were resistant to chloroquine.

RESULTS AND DISCUSSION

High degree of functional redundancy among *Plasmodium* hemoglobinases

To determine the essential nature of individual enzymes involved in *P. berghei* Hb digestion, we performed a loss-of-function analysis on eight predicted *P. berghei* hemoglobinases. The selection was based on the corresponding *P. falciparum* orthologous proteases with a characterized role in Hb digestion and/or located in the digestive vacuole (DV; Table S1 and Fig. 1 A). These include the aspartic protease, plasmepsin 4 (PM4), a single enzyme equivalent to the 4 *P. falciparum* plasmepsins (PM1–4); berghepain-2 (BP2), equivalent to the 2 *P. falciparum* DV falcipains FP-2 and FP-3; bergheilysin (BLN), the ortholog of *P. falciparum* falcilysin; dipetidyl peptidase 1 (DPAP1); and 4 aminopeptidases (aminopeptidase P [APP], M1-family alanyl aminopeptidase [AAP], M17-family leucyl aminopeptidase [LAP], and M18-family aspartyl aminopeptidase [DAP]). In addition, we included heme detoxification protein (HDP) and 3 enzymes related to DV proteases with undefined roles in Hb digestion (berghepain 1, the ortholog of *P. falciparum* falcipain 1 and 2 dipetidyl peptidases, DPAP2 and DPAP3). We successfully generated gene-deletion mutants for *pm4*, *bp1*, *bp2*, *dpap1*, *dpap2, dpap3*, *app*, *lap*, and *dap*; however, multiple attempts to disrupt *bln*, *aap*, and *hdp* were unsuccessful (Table S2). We previously reported that disruption of *pm4* in *P. berghei* results in the lack of all aspartic protease activity in the DV (Spaccapelo et al., 2010). Similarly, *P. falciparum* has been shown to survive without DV PM activity (Bonilla et al., 2007). We were able to generate mutants lacking BP2, whereas *P. falciparum* blood stages survive without FP2 but not FP3 (Sijwali et al., 2006). We also generated mutants that lack genes encoding DPAP1, APP, and LAP, whereas *P. falciparum* orthologs have been reported to be refractory to disruption (Table S1; Klemba et al., 2004; Dalal and Klemba, 2007). We were unable to select parasites lacking expression of AAP and BLN, and the *P. falciparum* orthologous genes *aap* and *bln* have also been reported to be resistant to disruption and shown to play additional roles outside DV (Dalal and Klemba, 2007; Ponpuak et al., 2007). We were also unable to select mutants lacking HDP expression, suggesting an essential role for *P. berghei* blood stages, as has been proposed for *P. falciparum* HDP (Jani et al., 2008). The successful deletion of 6 of the 8 genes encoding hemoglobinase indicates a high level of redundancy in vivo among these enzymes.

Mutants lacking PM4, DPAP1, BP1, LAP or APP exhibited a significant reduction in asexual multiplication rates (growth rates) compared with WT parasites, whereas growth rates of the other 4 mutants were not significantly reduced (Table 1). In addition, Δ*pm4* and Δ*app* mutants showed a significant reduction in Hz production quantified in mature schizonts (Sz; 8–24 nuclei) using reflection contrast polarized light microscopy (Fig. 1, A and B). Trophozoites (Tz) of Δ*app* and Δ*pm4* have an aberrant morphology as visible on Giemsa-stained smears, exhibiting an accumulation of translucent vesicles inside their cytoplasm (Fig. 1 C). The reduced Hz production in Δ*pm4* and Δ*app* mutants indicate that *P. berghei* blood stages can develop into mature Sz despite significantly reduced Hb digestion. The lower growth rate of mutants lacking downstream hemoglobinases DPAP1 and LAP (but with WT Hz levels) indicates that these enzymes are either important in effectively releasing amino acids from Hb peptides or that they have additional functions. Parasites lacking APP unexpectedly also had reduced levels of Hz. However, both APP and LAP are shown to have additional roles, e.g., in cytosolic peptide turnover (Dalal and Klemba, 2007). Although it remains to be investigated, APP may have an indirect effect on the initial steps of Hb digestion, either resulting from its involvement in establishment of the DV or due to feedback mechanisms that inhibit Hb digestion in the absence of APP.

Parasites lacking both PM4 and BP2 are restricted to reticulocytes and produce smaller Szs with less merozoites

Because in *P. berghei* PM4 is the only DV aspartic protease and BP2 is the single syntenic ortholog of the two *P. falciparum*

Downloaded from jem.rupress.org on June 23, 2015

Published May 4, 2015

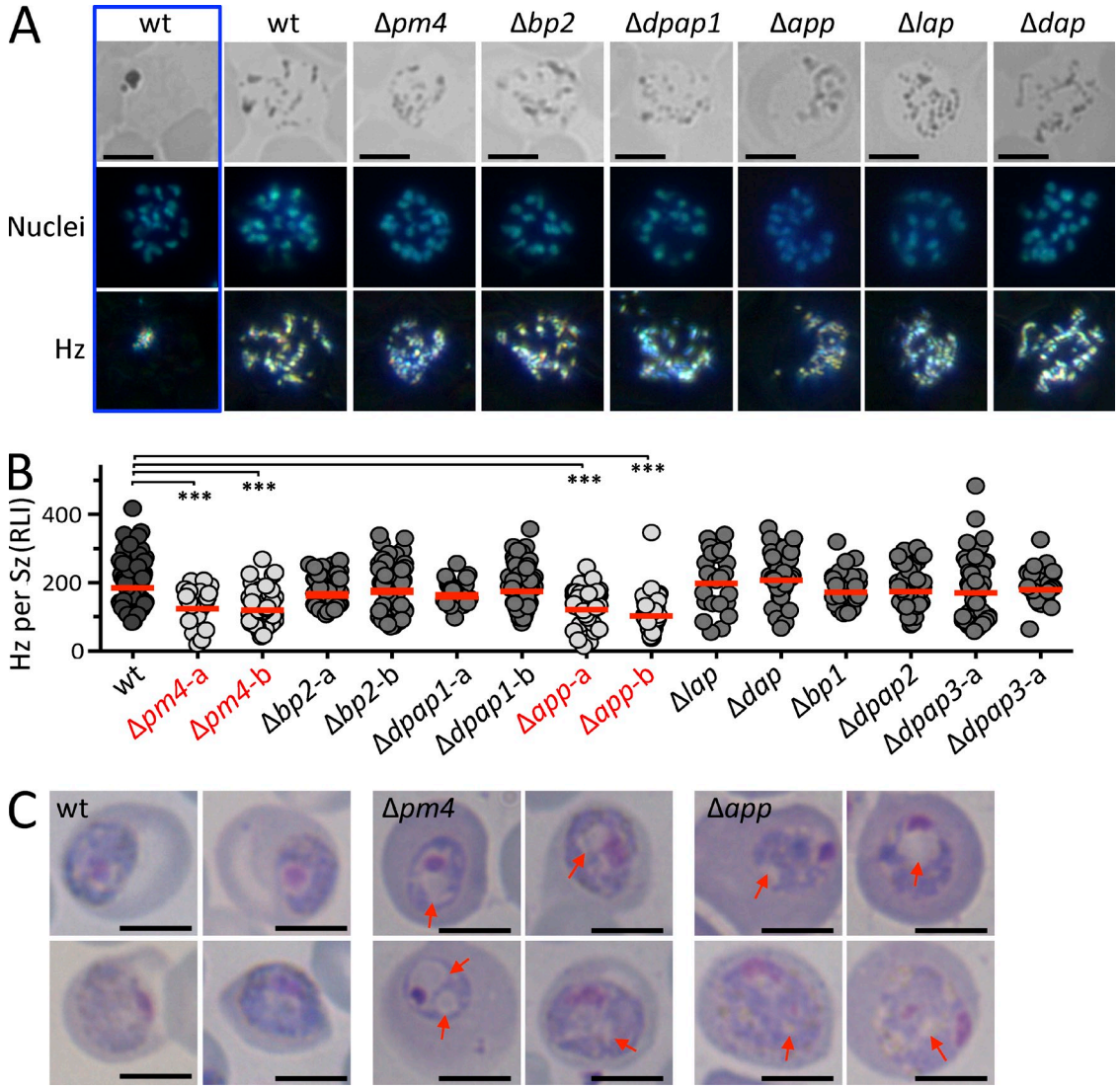

Figure 1. Δ*pm4* and Δ*app* parasites show reduced Hz levels and an aberrant morphology. (A) Reflection contrast polarized light microscopy was used to quantify Hz production inside an iRBC; representative images of Hz in mature Szs are shown. Hz crystals are scattered in Szs and were used for Hz quantification; a single Hz cluster is only observed in fully segmented Szs (blue box); BF, bright field; bars, 5 µm. (B) Relative light intensity (RLI) of polarized light was measured for individual Szs ($n > 30$; Student's *t* test; ***, $P < 0.0001$). (C) Aberrant morphology of Δ*pm4* and Δ*app* Tzs exhibiting reduced Hz production and an accumulation of translucent vesicles (indicated by arrows) in their cytoplasm. Bars, 5 µm. The phenotype was confirmed with two independent mutants.

DV cysteine endoproteases (FP-2 and FP-3), the absence of these enzymes is expected to result in the failure to proteolyse native Hb. Unexpectedly, we were able to generate two independent mutants lacking expression of both PM4 and BP2 (Δ*pm4*Δ*bp2*; Table S2). Blood stages of Δ*pm4*Δ*bp2* have a severely reduced multiplication rate (2.2–4.6 compared with WT rates of 10; Table 1). After an initial slow rise of parasite numbers in Δ*pm4*Δ*bp2*-infected mice, parasitemia can reach levels of up to 50% when mice became anemic and the RBCs were principally reticulocytes (unpublished data). At high parasitemias, mature Sz were present in the blood, most of which contained 8–12 merozoites (Fig. 2 A). Even though ring forms of Δ*pm4*Δ*bp2* were observed in both mature RBCs and reticulocytes, mature Tz and Sz were exclusively found in reticulocytes (unpublished data), indicating that Δ*pm4*Δ*bp2* parasites, while retaining their ability to invade all RBCs, are unable to develop in normocytes. This may be related to greater abundance/diversity of amino acids and proteins present in reticulocytes (Allen, 1960), or due to other physical characteristics of reticulocytes, for example, their larger size and reduced Hb content may provide more space for growth in the absence of Hb digestion.

Analysis of Giemsa-stained images revealed Δ*pm4*Δ*bp2*-Sz to be small, occupying only 25–65% of the RBCs, compared with 60–90% of WT Sz ($n > 30$; Fig. 2 A). This size reduction was confirmed by ImageStream flow cytometry on

Downloaded from jem.rupress.org on June 23, 2015

Published May 4, 2015

Table 1. Growth and virulence characteristics of blood stages of gene deletion mutants

Gene deletion mutant	Day to 0.5–2% parasitemia[a]	Multiplication rate[b]	Hz production[c]
WT[d]	8 (0.2); *n* = 40	10.0 (0.7)	198.8 (69.8)
Δ*pm4*-a[e]	9-11; *n* > 10	5.8 (0.5)-7.0 (1.0)[f]	129.5 (41.7)[f]
Δ*pm4*-b	9 (0); *n* = 2	7.7 (0)[f]	134.5 (47.6)[f]
Δ*bp2*-a	8 (0); *n* = 5	10.0 (0)	177.5 (45.1)
Δ*bp2*-b	8 (0); *n* = 6	10.0 (0)	188.4 (71.5)
Δ*dpap1*-a	9.5 (0.7); *n* = 2	7.0 (1.0)[f]	174.6 (34.0)
Δ*dpap1*-b	9 (0); *n* = 4	7.7 (0)[f]	189.2 (62.7)
Δ*app*-a	12 (0); *n* = 1	4.6 (0)[f]	131.8 (50.5)[f]
Δ*app*-b	12 (0); *n* = 4	4.6 (0)[f]	111.4 (49.7)[f]
Δ*dap*	8 (0); *n* = 3	10.0 (0)	223.8 (65.7)
Δ*lap*	15.5 (0.7); *n* = 2	3.3 (0.2)[f]	213.6 (78.7)
Δ*bp1*-a	9.7 (0.6); *n* = 3	6.8 (0.8)[f]	186.2 (49.2)
Δ*bp1*-b	9 (0); *n* = 1	7.7 (0)[f]	n.d.
Δ*dpap2*	8.3 (0.4); *n* = 4	9.4 (1.0)	187.8 (64.6)
Δ*dpap3*-a	8.3 (0.6); *n* = 3	9.2 (1.3)	184.5 (86.3)
Δ*dpap3*-b	8 (0); *n* = 5	10.0 (0)	193.3 (46.8)
Δ*pm4*Δ*bp2*-a	12, 16, 20; *n* = 3	3.4 (1.1)[f]	27.2 (36.5)[f]
Δ*pm4*Δ*bp2*-b	21, 24; *n* = 2	2.3 (0.1)[f]	46.1 (51.2)[f]

n.d., not determined.
[a]The day on which the parasitemia reaches 2–5% in mice infected with a single parasite in cloning assays. The mean of one cloning experiment and standard deviation are shown (*n* = the number of mice). For the Δ*pm4*Δ*bp2* mutants, the days for individual clones are shown.
[b]The multiplication rate (mean and SD) of asexual blood stages per 24 h, calculated based on the "day to 0.5–2% parasitemia" in the cloning assay.
[c]Relative light intensity (mean and SD) of Hz crystals in individual Szs, determined by polarized light microscopy. See Fig.1.
[d]WT, wild type *P. berghei* ANKA reference lines (cl15cy1, 676m1cl1, and 1037cl1). Data from >10 independent experiments.
[e]*pm4* gene-deletion mutants generated by Spaccapelo et al. (2010).
[f]$P < 0.0001$; Student's *t* test.

live WT and Δ*pm4*Δ*bp2* Szs expressing GFP under the control of the Sz-specific *ama-1* promoter (Fig. 2 B). Analysis of Giemsa-stained parasites indicated that Δ*pm4*Δ*bp2* Szs had fewer merozoites (Fig. 2 A). Measuring GFP and Hoechst fluorescence intensity by ImageStream and standard flow cytometry confirmed that mature Δ*pm4*Δ*bp2*-Sz have 40% reduction in both total DNA and (*ama1*-based) GFP expression levels compared with WT Sz, indicating a significant reduction in the total number of merozoites per Sz (Fig. 2, C and D). Combined, these observations demonstrate that Δ*pm4*Δ*bp* parasites produce smaller Sz with less daughter merozoites than WT Sz.

Parasites lacking both PM4 and BP2 can form Szs in the absence of detectable Hz

Most Δ*pm4*Δ*bp2* Tzs have an amoeboid-like appearance with translucent vesicles inside their cytoplasm, and their Tzs and Szs have little or no visible Hz (Fig. 2 A). Ultrastructural analyses confirmed this, showing that Δ*pm4*Δ*bp2* Tzs contained a higher number of cytostomes or endocytic vesicles filled with material that had a structural appearance similar to RBC cytoplasm (Fig. 3 A). This indicates that the absence of PM4 and BP2 does not affect the uptake of Hb from the RBC cytoplasm. Electron microscopic images revealed that 37% of the Tzs contained dark-stained (electron-dense) vesicles that are completely absent from WT parasites (Fig. 3 A). These vesicles are very similar to those that have been described in *P. falciparum* Tz when Hb trafficking or digestion is blocked by inhibitors, and it has been proposed that these vesicles are cytostome derived and contain concentrated undigested and/or denatured Hb (Fitch et al., 2003; Vaid et al., 2010). In addition, although WT Tz contained large numbers of Hz crystals, >40% of Δ*pm4*Δ*bp2* Tz had no visible Hz crystals (Fig. 3 A), reflecting our observations with Giemsa-stained images of Tz and Sz (Fig. 2 A). Next, we used reflection contrast polarized light-microscopy to determine the amount of Hz in maturing Δ*pm4*Δ*bp2*-Sz and WT-Sz. The relative light intensity (RLI) values of Δ*pm4*Δ*bp2*-Sz at all stages of maturation were strongly reduced (78–87% reduction compared with WT Sz; Fig. 3 B and Table 1), and whereas all WT Sz had Hz, a large percentage (35–48%) of Δ*pm4*Δ*bp2*-Sz had no detectable Hz (Fig. 3 B), having RLI values the same as uninfected RBCs. The severe reduction in Hz production was also reflected in vastly reduced Hz deposition in organs of Δ*pm4*Δ*bp2*-infected mice compared with WT- and even Δ*pm4*-infected mice (Fig. 3 C).

We further quantified the amount of Hz and undigested Hb in equal numbers of FACS-purified Sz using heme-dependent luminol-enhanced luminescence analysis (Schwarzer et al., 1994). The Hb that remained undigested in Δ*pm4*Δ*bp2*-Sz iRBCs was twice the amount of that in WT-Sz iRBCs (Fig. 3 D); however, the total heme content in Δ*pm4*Δ*bp2*-Sz

Downloaded from jem.rupress.org on June 23, 2015

Published May 4, 2015

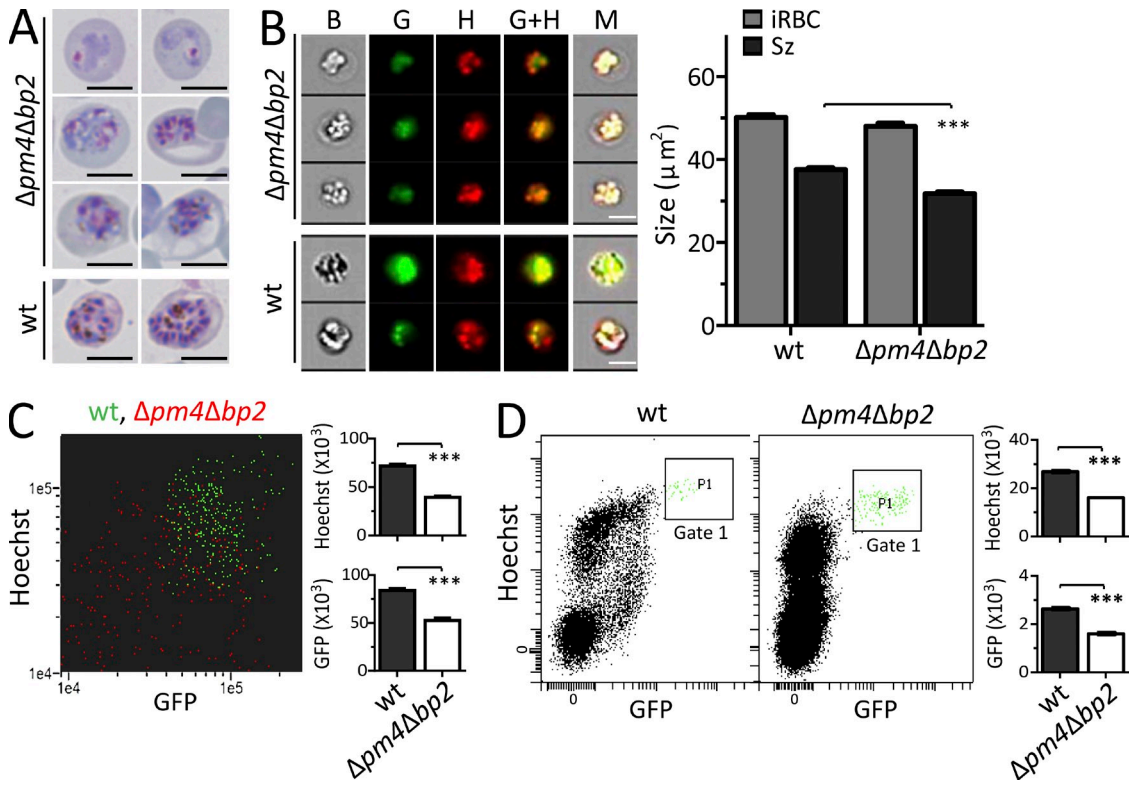

Figure 2. Szs of mutants lacking PM4 and BP2 expression are smaller in size and produce fewer merozoites. (A) Representative Giemsa-stained images showing the difference in size and merozoites production of Δ*pm4*Δ*bp2* iRBCs relative to WT. Bars, 5 µm. (B) Images of Hoechst stained mature WT and Δ*pm4*Δ*bp2* Szs expressing GFP under Sz-specific *ama1* promoter in their cytoplasm (right) and their size measurement by ImageStream flow cytometry (left). Bars, 5 µm. The size of individual iRBC was determined from bright field images (B) and the size of Sz was measured from the combined GFP (G) and Hoechst (H) images (i.e., G+H). M, merged images ($n > 250$; ***, $P < 0.0001$; Student's *t* test). (C) The dot plot (left) generated from ImageStream flow cytometry shows the GFP- and Hoechst-fluorescence of individual WT- (green) and Δ*pm4*Δ*bp2*- (red) Sz, and the GFP expression and DNA content were quantified (right). (D) The GFP and DNA content of mature Szs were measured by standard flow cytometry; mature Szs were selected in Gate 1 (left) and the quantification shown as bar graphs (right). All data are representative of two independent experiments (bar graphs show mean fluorescence intensity with SEM; ***, $P < 0.0001$; Student's *t* test).

iRBCs was 40% lower than WT-Sz iRBCs. On average, 54% (between 20–100%) of Hb remains undigested in Δ*pm4*Δ*bp2*-Sz iRBCs, compared with 12% of WT-Sz iRBCs (Fig. 3 D). Combined, the increased number of cytostome inclusions, presence of unusual electron-dense vesicles and severely reduced and often absent Hz crystals indicate that Hb digestion is severely impaired in Δ*pm4*Δ*bp2* and this is further supported by the high levels of undigested Hb present in RBCs infected with Δ*pm4*Δ*bp2* Sz compared with WT-Sz. However, some Hz is still present in a proportion of Δ*pm4*Δ*bp2* parasites indicating that some heme is released from Hb in the absence of PM4 and BP2. Whether this is the result of a compensatory enzymatic process or a nonspecific disassembly of the Hb tetramer that may occur when Hb accumulates in cytostomes or in the acidified dark-staining vesicles (Fitch et al., 2003) is unknown and requires further investigation.

In *P. falciparum* the PMs and FPs overlap in function and there is extensive functional redundancy within and between these two protease classes (Bonilla et al., 2007; Liu et al., 2006). Our observations on Hz production in the single gene-deletion mutants Δ*pm4* and Δ*bp2* indicate that also in *P. berghei* aspartyl and cysteine endopeptidases overlap in their ability to hydrolyze Hb. Interestingly, the Δ*bp2* mutant has a normal growth rate and produces WT levels of Hz, whereas Δ*pm4* parasites have a reduced growth and Hz production. These observations demonstrate that although PM4 is able to fully compensate for the function of BP2, BP2 can only partly compensate for the loss of PM4.

Gametocytes of parasite lacking both PM4 and BP2 are fertile despite their smaller size and reduced Hz levels

In mice infected with Δ*pm4*Δ*bp2* parasites, male and female gametocytes were readily detected. Similar to Sz, they were 23% smaller than WT gametocytes, and their cytoplasm had strongly reduced or no Hz crystals (Fig. 4 A). Most Δ*pm4*Δ*bp2* male gametocytes produced motile gametes (79.3 ± 4.6%), which are able to fertilize female gametes and produce ookinetes; these undergo meiosis and become tetraploid (Fig. 4, B and C). The conversion rates of Δ*pm4*Δ*bp2* female gametes into ookinetes were comparable to those of WT parasites (60.0 ± 6.1%; Fig. 4 C). Analysis of Hz levels in WT and Δ*pm4*Δ*bp2* ookinetes revealed that they also had reduced

Downloaded from jem.rupress.org on June 23, 2015

Published May 4, 2015

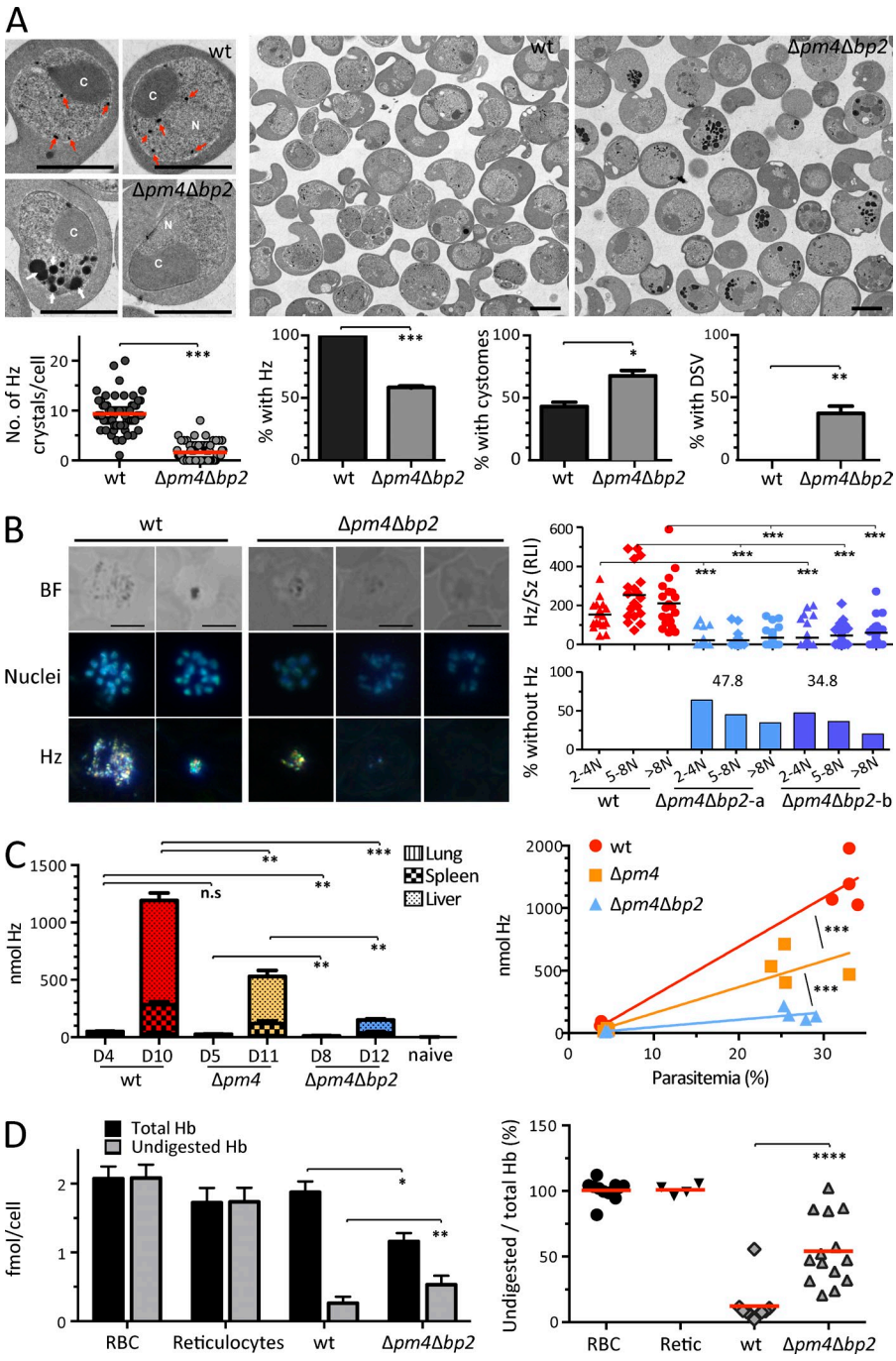

Figure 3. Δ*pm4*Δ*bp2* mutant parasites can develop into mature Szs with reduced Hb digestion and little or no detectable Hz. (A) Electron microscopy images of Δ*pm4*Δ*bp2* and WT-Tzs were used to identify and calculate the number of Hz crystals (red arrows), cytostomes (C), and dark-staining vesicles (DSV, white arrows) in WT and Δ*pm4*Δ*bp2* parasites. Data were obtained from 3 EM image fields ($n > 60$; ***, $P < 0.0005$; Student's *t* test). N, nucleus. Bars, 5 µm. (B) Reflection contrast polarized light microscopy was used to quantify Hz production in Δ*pm4*Δ*bp2* and WT Sz. Bright field (BF) and polarized light microscopy images showing Hz in individual representative Sz (left). Relative light intensity (RLI) of Hz crystals was measured in individual WT or Δ*pm4*Δ*bp2* Sz containing either 2–4, 5–8, or >8 nuclei (N; $n > 20$; ***, $P < 0.0005$; Student's *t* test; right). Bars, 5 µm. (C) Hz deposition in different organs of BALB/c mice infected with WT or Δ*pm4*Δ*bp2*-parasites at different days after infection was quantified. The deposition of Hz in different organs at different days (left; data presented as mean with SEM; $n = 4$) and the relationship between total Hz levels (nmol) quantified from all organs and peripheral parasitemias (right); **, $P < 0.05$; ***, $P < 0.0005$ (Student's *t* test). (D) Quantification of total Hb and undigested Hb, using heme-dependent, luminol-enhanced luminescence, in WT and Δ*pm4*Δ*bp2* Sz iRBCs; Hb and Hz levels in mature RBC and reticulocytes (left; data presented as mean with SEM) and the percentage of undigested Hb in these cells (right) are shown. *, $P < 0.05$; **, $P < 0.005$; ****, $P < 0.001$; Student's *t* test, $n > 3$. Data were pooled from three independent experiments.

Hz-levels (57%; Fig. 4 C). These observations demonstrate that both asexual and sexual blood-stages can complete development despite the severely impaired Hb digestion.

Parasites lacking both PM4 and BP2 are resistant to chloroquine but retain their sensitivity to artesunate

We tested the sensitivity of the Δ*pm4*Δ*bp2* parasites to artesunate (AS) and chloroquine (CQ); their mode of action is believed to depend on Hb digestion/Hz formation (Egan et al., 2004; Klonis et al., 2011). As a control we used sulfadiazine (SD), an inhibitor of folic acid synthesis (Kinnamon et al., 1976). AS and SD treatment of WT- and Δ*pm4*Δ*bp2*-infected BALB/c mice resulted in rapid clearance of parasites from bloodstream in 3–4 and 4–5 d after start of AS (50 mg/kg body weight, i.p.) and SD (35 mg/liter in drinking water) treatment, respectively (Fig. 5 A). Similarly, BALB/c mice infected with WT parasites rapidly cleared their infection after CQ (288 mg/liter in drinking water) treatment (3–4 d). In contrast, mice infected with pm4bp2 parasites, first exhibited an increase in parasitemia for 3 d, followed by a slow decline (Fig. 5 A). Parasites with normal morphology were present 6 d after start of CQ treatment (Fig. 5 B). Untreated

Downloaded from jem.rupress.org on June 23, 2015

Published May 4, 2015

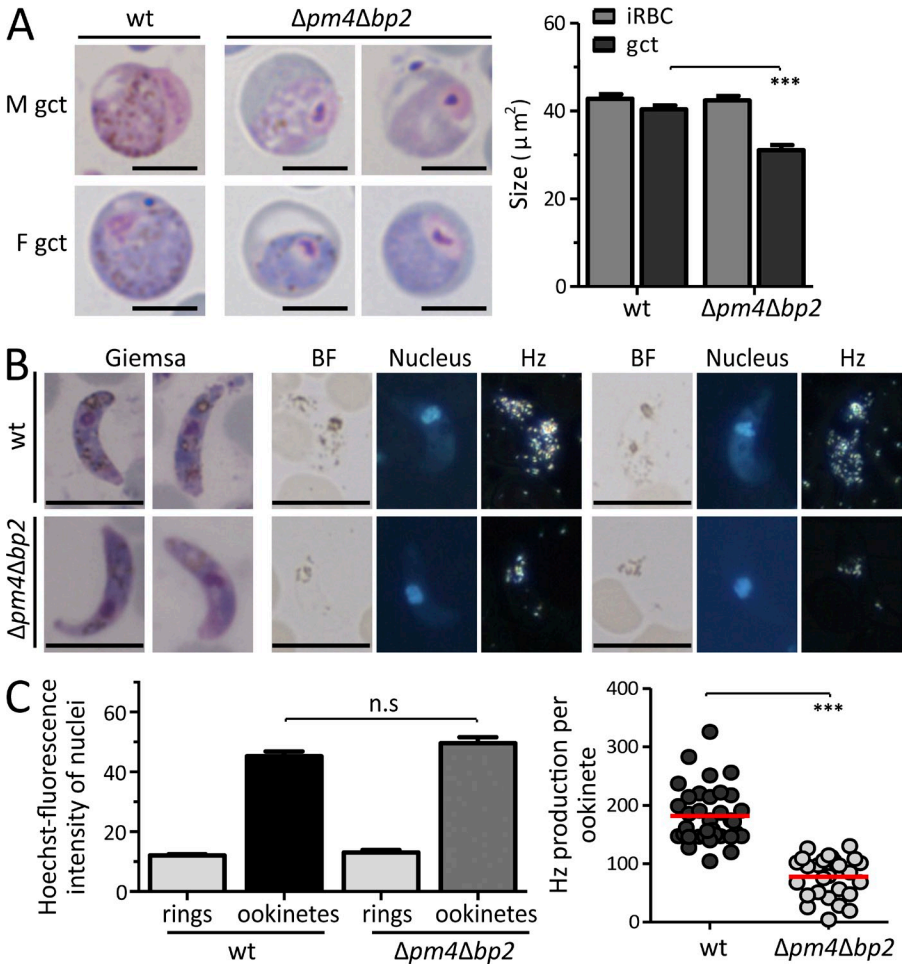

Figure 4. Gametocytes of Δ*pm4*Δ*bp2* are fertile despite their smaller size and reduced Hz production. (A) Representative Giemsa-stained images of WT and Δ*pm4*Δ*bp2* gametocytes (left; bars, 5 µm) and the size quantification on these images (right; $n > 30$; ***, $P < 0.0001$; Student's *t* test). (B) Giemsa-stained images and polarized light microscopy images of ookinetes. BF, bright-field; Nuclei (blue) stained with Hoechst. Bars, 5 µm. (C) Hoechst fluorescence intensity (DNA content) of WT and Δ*pm4*Δ*bp2* ookinetes, relative to haploid ring-form stages, was quantified (left; $n > 25$; n.s, not significant; Student's *t* test) indicating that both WT and Δ*pm4*Δ*bp2* ookinetes are tetraploid. Relative light intensity (RLI) of polarized light (Hz production) measurements of WT and Δ*pm4*Δ*bp2* ookinetes (right; $n > 25$; ***, $P < 0.0001$; Student's *t* test).

BALB/c mice also resolved a Δ*pm4*Δ*bp2* infection 3–4 wk after infection, indicating that host immunity may contribute to the decline of parasitemia in CQ-treated mice. We therefore performed infections and CQ treatment in Rag2$^{-/-}\gamma c^{-/-}$ mice (deficient in B, T, and NK cells). Whereas CQ-treated, WT-infected mice cleared a 2–5% WT infection within 3 d, in Δ*pm4*Δ*bp2*-infected mice parasites persisted for >20 d of CQ-treatment (Fig. 5 C), during which only Hz-negative Δ*pm4*Δ*bp2* parasites were observed in circulation (Fig. 5 D). To examine whether Δ*pm4*Δ*bp2* parasite resistance to CQ is lost at higher concentrations of CQ and conversely if resistance to AS is observed at lower concentrations of AS, we performed drug sensitivity assays using 5 and 10 mg/kg AS (in BALB/c mice) or with 600 mg/liter CQ (in Rag2$^{-/-}\gamma c^{-/-}$ mice). These experiments revealed that, at lower AS doses, drug sensitivity does not significantly differ between Δ*pm4*Δ*bp2* and WT parasites, and that Δ*pm4*Δ*bp2* parasites are resistant to CQ even at high doses (Fig. 5 E).

Our observations on the ability of *Plasmodium* parasites to develop without detectable Hz formation that are resistant to CQ indicate a novel mechanism of resistance against drugs that target Hb proteolysis. Interestingly, previous studies on CQ-resistant *P. berghei* lines revealed that parasites are more restricted to development in reticulocytes and produced less Hz (Platel et al., 1999). It has been proposed that CQ-resistance of parasites with reduced Hz is due to detoxification of hemin by elevated levels of glutathione in parasites inside reticulocytes, thus precluding heme-polymerization and preventing CQ activity (Platel et al., 1999; Fidock and DeSilva, 2012). However, our observations may provide a more direct explanation for CQ-resistance and reduced Hz production in these parasites, namely that these parasites, like the Δ*pm4*Δ*bp2*, digest less Hb in reticulocytes.

Our observations may have particular relevance for the human malaria parasite, *Plasmodium vivax*, which is also reticulocyte-restricted. *P. vivax* CQ resistance appears to be different from *P. falciparum* (Suwanarusk et al., 2007; Baird et al., 2012), and no clear association has been found with mutations in the same genes that typify *P. falciparum* CQ resistance (*pfcrt* or *pfmdr1*). In addition, DV formation in *P. vivax* appears to resemble more DV formation in *P. berghei* than in *P. falciparum*. Tzs of *P. falciparum* have a large central DV, as Hb-containing cytostomes merge rapidly and Hz formation occurs principally in this single DV. In contrast, *P. berghei* has many small Hb-containing vesicles, in which Hb digestion/Hz formation occurs, resulting in scattered Hz granules throughout

Downloaded from jem.rupress.org on June 23, 2015

Published May 4, 2015

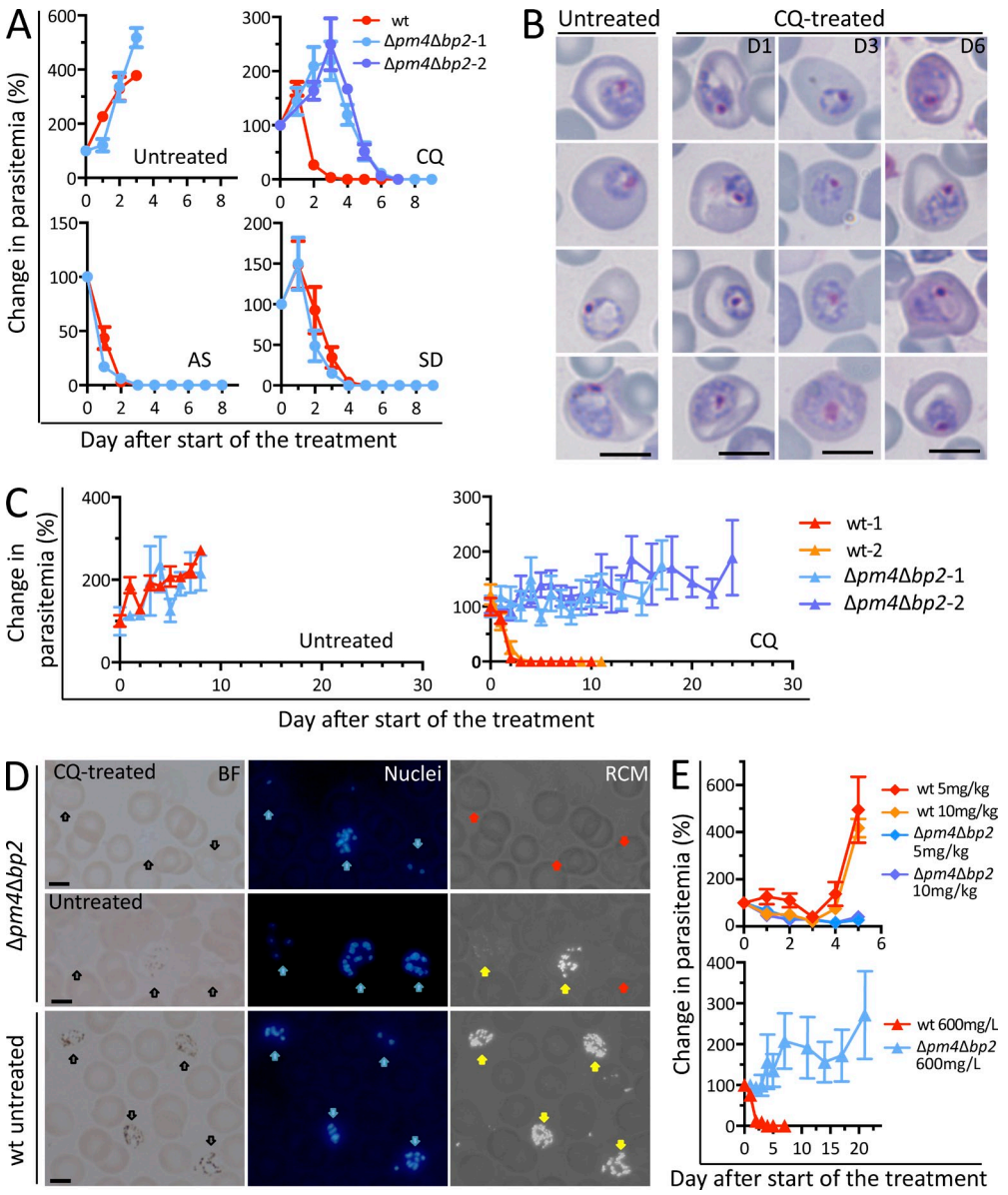

Figure 5. Δ*pm4*Δ*bp2* parasites are resistant to chloroquine but sensitive to artesunate. (A) Changes in parasitemia of BALB/c mice ($n = 5$) infected with WT or Δ*pm4*Δ*bp2* parasites after treatment with chloroquine (CQ; 288mg/liter in drinking water; 2 experiments), artesunate (AS; 50 mg/kg body weight i.p), or sulfadiazine (SD; 35 mg/liter in drinking water). Data presented as mean with SEM. (B) Representative Giemsa-stained images of *pm4*Δ*bp2*-Tzs in blood of BALB/c mice treated with CQ treatment at different days (D1, 3, 6) after start of CQ treatment. Bars, 5 µm. (C) Changes in parasitemia of Rag2$^{-/-}$γc$^{-/-}$ ($n = 6$) mice infected with WT or Δ*pm4*Δ*bp2* parasites either without treatment (left) or after prolonged CQ treatment (right; 288 mg/l in drinking water; 2 experiments). (D) Reflection contrast polarized light microscopy images (RCM) showing the absence of Hz crystals in Δ*pm4*Δ*bp2* parasites that survived CQ treatment for >20 d in Rag2$^{-/-}$γc$^{-/-}$ mice; iRBC with no Hz formation are indicated by red arrows. In untreated mice, two populations of Δ*pm4*Δ*bp2* parasites are present, parasites with no Hz (red arrow), and parasites with Hz crystals (yellow arrows). WT parasites in untreated mice show large amounts of Hz (yellow arrows). Black arrows indicate iRBC in bright field (BF) images. Nuclei of parasites (blue) were stained with Hoechst (blue arrows). Bars, 5 µm. (E) Changes in parasitemia of BALB/c mice (top, $n = 5$) or Rag2$^{-/-}$γc$^{-/-}$ mice (bottom, $n = 5$) infected with Δ*pm4*Δ*bp2* and WT parasites exposed to either 5 or 10 mg/kg of AS in or to 600 mg/l CQ in drinking water. Data presented as mean values of changes (%) in parasitemia with SEM.

the cytoplasm of the parasite, these clusters coalesce when schizogony starts (Slomianny et al., 1985). It has been suggested that the uptake of Hb from reticulocytes by the process of micropinocytosis results in multiple small vesicles containing Hb and Hz in both *P. berghei* and *P. vivax* (Jeffers, 2010). Moreover *P. vivax*, like *P. berghei*, has only 1 DV plasmepsin (PM4) in contrast to *P. falciparum* which encodes 4 DV plasmepsins (Table S1). While *P. vivax* has 3 DV vivapains, 2 of them, VX2 and 3, are syntenic orthologs of FP-2 and 3 the other, VX4, is nonsyntenic with the FPs but shows greater

Downloaded from jem.rupress.org on June 23, 2015

Published May 4, 2015

sequence similarity to BP2 (Na et al., 2010; Table S1). These observations indicate that mechanisms of Hb uptake and digestion in *P. vivax* more closely resembles *P. berghei* than *P. falciparum* and future research is required to see if this also translates into similar mechanisms to resistance to drugs that exclusively target Hb digestion pathways.

Although Δ*pm4*Δ*bp2* parasites are resistance to CQ, they retain sensitivity to AS. Although the precise mode of action of artemisinin and related derivatives remains contentious, it is believed that their activity results from activation by reduced heme iron in the DV (Eastman and Fidock, 2009). Our results suggest AS activity is not affected by reduced Hb digestion or absence of Hz formation. Alternatively AS activation in Δ*pm4*Δ*bp2* parasites in reticulocytes may derive from a labile pool of heme that exists in reticulocytes for Hb synthesis. *P. vivax* resistance to artemisinins has not been reported; however, most of the artemisinin-based combination therapies have proven efficacy against chloroquine-resistant strains of *P. vivax* (Price et al., 2014).

We show that, very much counter to expectation, Hb digestion and Hz formation appears not to be essential to parasite survival when parasites develop in reticulocytes. Indeed, our findings support the notion that *Plasmodium* parasites retain multiple modes of development and survival during blood stage development, which has important implications for antimalarial drug design, in particular drugs that target Hb digestion and Hz formation.

MATERIALS AND METHODS

Experimental animals and parasites. Female C57BL/6, BALB/c, Swiss OF1 mice (6–8 wk old; Charles River) and female Rag2$^{-/-}\gamma c^{-/-}$ mice (6–8 wk old, bred in MRC NIMR) were used. All animal experiments performed at the Leiden University Medical Center (LUMC) were approved by the Animal Experiments Committee of the LUMC (DEC 10099; 12042; 12120). All animal experiments performed at the University of Perugia were approved by Ministry of Health under the guidelines D.L. 116/92). All animal experiments performed in MRC NIMR were performed after review and approval by the MRC National Institute for Medical Research Ethical Review Panel in strict accordance to current UK Home Office regulations, and conducted under the authority of UK Home Office Project License PPL 80/2358. The Dutch, Italian, and British Experiments on Animal Act were established under European guidelines (EU directive no. 86/609/EEC regarding the Protection of Animals used for Experimental and Other Scientific Purposes).

Two reference *P. berghei* ANKA parasite lines were used: line cl15cy1 (WT) and reporter line 1037cl1 (WT-GFP-Luc$_{schiz}$; mutant RMgm-32). This reporter line contains the fusion gene *gfp-luc* gene under control of the Sz-specific *ama1* promoter integrated into the silent *230p* gene locus (PBANKA_030600) and does not contain a drug-selectable marker (Spaccapelo et al., 2010).

Generation of *P. berghei* mutants. DNA constructs used to disrupt genes were based on the standard plasmids (pL0001 [MRA-770], pLTgDFHR, and pL0035; [MRA-850]) and by modified PCR methods based on pL0040 and pL0048 (Lin et al., 2011). Targeting sequences for homologous recombination were PCR amplified from *P. berghei* ANKA (cl15cy1) genomic DNA using primers specific for the 5′ or 3′ end of each gene using primer sets of P1/P2, P3/P4, respectively (see Table S3 for the primer sequences).

The DNA construct targeting *bp1* was provided by P. Sinnis (Johns Hopkins University, Baltimore, MD). Transfection, selection, cloning, and genotyping of transformed parasites was performed using standard genetic modification technologies for *P. berghei* (Janse et al., 2006). To generate Δ*pm4*Δ*bp2* mutant, h*dhfr*::y*fcu* selectable marker was removed by negative selection (Braks et al., 2006) from Δ*bp2*-b (based on pL0035) and *pm4* gene was subsequently targeted in Δ*bp2*-b^{-sm} line. Table S2 provides details of all gene deletion experiments, such as experiment number, targeting construct, parental line for transfection, and RMgmDB IDs (Rodent Malaria Genetically Modified Parasites Database). Details for targeting construct generation (maps and sequences) and genotyping results can be found in RMgmDB and Table S4 includes primers used for genotyping including diagnostic PCR, Southern analyses of chromosomes separated by pulsed-field gel electrophoresis, Northern PCR, and RT-PCR.

In vivo asexual multiplication (growth) rates. The multiplication (growth) rate of asexual blood-stages in mice was determined during cloning of the gene-deletion mutants as described before (Spaccapelo et al., 2010) and was calculated as follows: the percentage of infected erythrocytes (parasitemia) in Swiss OF1 mice injected with a single parasite was determined by counting Giemsa-stained blood films when parasitemias reach 0.5–2%. The mean asexual multiplication rate per 24 h was then calculated assuming a total of 1.2×10^{10} erythrocytes per mouse (2 ml of blood). The percentage of infected erythrocytes in mice infected with reference lines of the *P. berghei* ANKA strain consistently ranged between 0.5–2% at day 8 after infection, resulting in a mean multiplication rate of 10 per 24 h.

Gametocyte and ookinete production. Gametocyte production is defined as the percentage of ring forms developing into mature gametocytes during synchronized infections (Janse and Waters, 1995). Male gamete production (exflagellation) and ookinete production was determined in standard in vitro fertilization and ookinete maturation assays (Janse and Waters, 1995); ookinete production is defined as the percentage of female gametes that develop into mature ookinetes under standardized in vitro culture conditions. Female gamete and mature ookinete numbers were determined on Giemsa-stained blood smears made 16–18 h after activation. Hz level of ookinetes were quantified.

Sz and gametocyte size measurements. For the Giemsa-stained smears, pictures were taken using a Leica microscope from randomly chosen fields of 300–400 RBCs, and all iRBCs were measured in these fields. The sizes of iRBCs and the parasites were measured by ImageJ by gating on the areas of parasites and iRBC. For ImageStream flow cytometry analysis, iRBCs containing Szs of WT-GFP-Luc$_{schiz}$ and Δ*pm4*Δ*bp2* parasites were collected from infected BALB/c mice with a high parasitemia (10–30%) and enriched by Nycodenz density centrifugation (Janse et al., 2006). Purified parasites were then collected in complete RPMI-1640 culture medium and stained with Hoechst-33258 (2 µmol/liter; Sigma-Aldrich) for 1 h at room temperature. Cultured, mature Szs of WT *P. berghei* ANKA (cl15cy1) were used as unstained control; Hoechst stained cl15cy1 (Hoechst only) and nonstained WT-GFP-Luc$_{schiz}$ (GFP only) were used as single-color controls. The analyses were performed using an Amnis ImageStream X imaging cytometer (Amnis Corp.) and images were analyzed using the IDEAS image analysis software.

Hz and Hb quantification. Hz was quantified in Szs using different methods. Hz was quantified by measuring the relative light intensity (RLI) of Hz crystals in Szs and ookinetes by reflection contrast polarized light microscopy. Szs were either collected from overnight in vitro blood stage cultures or directly from tail blood when Szs were present in the peripheral circulation. Blood smears were made from cultured parasites or from tail blood and stained with Hoechst-33342 (2 µmol/liter; Sigma-Aldrich) for 20 min. Szs (8–24 nuclei) with scattered Hz were selected and pictures were taken with a LeicaDM/RB microscope (Leica) which was adapted for reflection contrast polarized light microscopy (Cornelese-ten Velde et al., 1988). The RLI of Hz crystals in the Szs was measured using ImageJ software (NIH).

In addition, Hb and Hz from WT and Δ*pm4*Δ*bp2* Sz-iRBC were quantified by measuring the heme-dependent luminol-enhanced luminescence (Schwarzer et al., 1994). For these experiments, 10^4 purified Szs were collected by flow sorting from infected blood of BALB/c mice with a high parasitemia

Downloaded from jem.rupress.org on June 23, 2015

Published May 4, 2015

(10–30%) and stained with Hoechst-33258 (2 µmol/liter; Sigma-Aldrich) at 37°C in the dark for 1 h. Subsequently, Szs were selected and sorted with a FACSAria II cell sorter (BD; speed 10,000 events/s). Mature Szs were selected by gating on the GFP^+ population of cells with a DNA content of Szs (Hoechst fluorescence intensity 8–24 N; Fig. 2 D, gate 1). Purified Szs were washed with PBS and concentrated in 10 µl of PBS and kept at −80°C until further analysis. Szs were analyzed for their Hb and Hz content. Hb-bound heme and alkali-solubilized Hz-heme were assayed by luminol-enhanced luminescence in the untreated or strong alkali-treated lysates prepared as detailed previously (Schwarzer et al., 1994).

To quantify Hz deposition in organs of infected mice, groups of 8 BALB/c mice were i.p. infected with 10^5 WT, Δ*pm4*, or Δ*pm4*Δ*bp2* parasites. At different parasitemias, mice were sacrificed and systemically perfused with 20 ml PBS to remove circulating iRBC from the organs. Livers, spleens, and lungs were removed, weighed and stored at −80°C until further analysis. The Hz extraction from these organs and quantification was performed using an optimized method for Hz quantification in tissues as described (Deroost et al., 2012).

Electron microscopy analysis. Infected blood was collected from WT or Δ*pm4*Δ*bp2* parasite infected BALB/c mice by heart puncture and enriched by Nycodenz centrifugation (Janse et al., 2006). IRBC (10^7–10^8) were collected and fixed overnight in 2 ml of 1.5% glutaraldehyde in 0.1 M sodium cacodylate. After centrifugation, the pellet was rinsed twice with 0.1 M sodium cacodylate and postfixed with 1% osmium tetroxide in 0.1 M sodium cacodylate. After rinsing, samples were dehydrated in a graded ethanol series up to 100% and embedded in epon. 110-nm sections were cut with a microtome and transferred onto standard grids and post-stained with uranyl acetate and lead citrate. Transmission electron microscopy (TEM) data were collected on a FEI Tecnai microscope at 120 kV with a FEI Eagle CCD camera. Virtual slides (Faas et al., 2012) consisting of 759 and 729 unbinned 4kx4k images were collected for the WT and Δ*pm4*Δ*bp2* sample, respectively. The magnification at the detector plane was 12930: the pixel size 1.2 nm square. The resulting slides cover an area of 109 × 105 μm^2 and 105 × 105 μm^2 for the respective samples. The virtual slides were analyzed by Aperio ImageScope software (Aperion). All statistical tests were performed using GraphPad Prism.

Drug sensitivity assays. Groups of 5–6 BALB/c or $Rag2^{-/-}\gamma c^{-/-}$ mice were i.p. infected with either 10^4 WT or 10^5 Δ*pm4*Δ*bp2*-parasites. At a peripheral parasitemia of 2–5%, mice were treated with artesunate (AS; Pharbaco; 60 mg powder [a gift from Dafra Pharma International, Turnhout, Belgium], chloroquine [CQ; Sigma-Aldrich], or sulfadiazine [SD; Sigma-Aldrich]) and parasitemia was monitored daily by counting Giemsa-stained blood films of tail blood. AS treatment was performed by i.p. injection of 6.25, 1.25, or 0.625 mg/ml in 5% $NaHCO_3$ as a single dose for 4 consecutive days (50, 10, or 5 mg/kg body weight). SD was provided at a concentration of 35 mg/liter in drinking water for 7 d, and CQ was provided at a concentration of 288 or 600 mg/liter with 15 g/liter glucose in the drinking water for a period of 7 d in BALB/c or up to 25 d in $Rag2^{-/-}\gamma c^{-/-}$ mice. The parasitemia was monitored every 1–2 d by Giemsa-stained thin blood smears. All infected mice were sacrificed when the parasitemia reached 50%.

Graphs and statistical analyses. All graphs and statistical analyses were made in GraphPad Prism, all error bars indicate SEM and all p-values were derived from unpaired Student's *t* tests.

Supplemental material. Table S1 shows genes targeted in this study. Table S2 shows details of transfection experiments aiming at deletion of *P. berghei* genes encoding hemoglobinases. Table S3 shows gene deletion constructs and primers. Table S4 shows primers for genotyping gene-deletion mutants. Online supplemental material is available at http://www.jem.org/cgi/content/full/jem.20141731/DC1.

We would like to thank Dr. Photini Sinnis for providing us with a *P. berghei bp1* gene deletion construct, J.J. Onderwater for electron microscopy sample preparation, and Guido de Roo and Sabrina Veld for assistance with flow cytometry experiments.

J.-w. Lin was supported by the China Scholarship Council-Leiden University Joint Program and C.J. Janse by a grant of the European Community's Seventh Framework Programme (FP7/2007–2013) under grant agreement no. 242095. K. Deroost was supported by a PhD grant of the Agency for Innovation by Science and Technology (IWT), and P.E. Van den Steen was supported by a grant of the "Geconcerteerde OnderzoeksActies" (GOA 2013/014) of the Research Fund of the KU Leuven, and by the Fund for Scientific Research (F.W.O.-Vlaanderen). J. Langhorne is supported by the MRC, UK (U117584248).

The authors declare no competing financial interests.

Submitted: 7 September 2014
Accepted: 8 April 2015

REFERENCES

Allen, D.W. 1960. Amino acid accumulation by human reticulocytes. *Blood*. 16:1564–1571.

Baird, J.K. 2004. Chloroquine resistance in Plasmodium vivax. *Antimicrob. Agents Chemother.* 48:4075–4083. http://dx.doi.org/10.1128/AAC.48.11.4075-4083.2004

Baird, K.J., J.D. Maguire, and R.N. Price. 2012. Diagnosis and treatment of Plasmodium vivax malaria. *Adv. Parasitol.* 80:203–270. http://dx.doi.org/10.1016/B978-0-12-397900-1.00004-9

Bonilla, J.A., T.D. Bonilla, C.A. Yowell, H. Fujioka, and J.B. Dame. 2007. Critical roles for the digestive vacuole plasmepsins of Plasmodium falciparum in vacuolar function. *Mol. Microbiol.* 65:64–75. http://dx.doi.org/10.1111/j.1365-2958.2007.05768.x

Braks, J.A., B. Franke-Fayard, H. Kroeze, C.J. Janse, and A.P. Waters. 2006. Development and application of a positive-negative selectable marker system for use in reverse genetics in Plasmodium. *Nucleic Acids Res.* 34:e39. http://dx.doi.org/10.1093/nar/gnj033

Cornelese-ten Velde, I., J. Bonnet, H.J. Tanke, and J.S. Ploem. 1988. Reflection contrast microscopy. Visualization of (peroxidase-generated) diaminobenzidine polymer products and its underlying optical phenomena. *Histochemistry*. 89:141–150.

Dalal, S., and M. Klemba. 2007. Roles for two aminopeptidases in vacuolar hemoglobin catabolism in Plasmodium falciparum. *J. Biol. Chem.* 282:35978–35987. http://dx.doi.org/10.1074/jbc.M703643200

Deroost, K., N. Lays, S. Noppen, E. Martens, G. Opdenakker, and P.E. Van den Steen. 2012. Improved methods for haemozoin quantification in tissues yield organ-and parasite-specific information in malaria-infected mice. *Malar. J.* 11:166. http://dx.doi.org/10.1186/1475-2875-11-166

Eastman, R.T., and D.A. Fidock. 2009. Artemisinin-based combination therapies: a vital tool in efforts to eliminate malaria. *Nat. Rev. Microbiol.* 7:864–874. http://dx.doi.org/10.1038/nrmicro2239

Egan, T.J., K.R. Koch, P.L. Swan, C. Clarkson, D.A. Van Schalkwyk, and P.J. Smith. 2004. In vitro antimalarial activity of a series of cationic 2,2′-bipyridyl- and 1,10-phenanthrolineplatinum(II) benzoylthiourea complexes. *J. Med. Chem.* 47:2926–2934. http://dx.doi.org/10.1021/jm031132g

Elliott, D.A., M.T. McIntosh, H.D. Hosgood III, S. Chen, G. Zhang, P. Baevova, and K.A. Joiner. 2008. Four distinct pathways of hemoglobin uptake in the malaria parasite Plasmodium falciparum. *Proc. Natl. Acad. Sci. USA*. 105:2463–2468. http://dx.doi.org/10.1073/pnas.0711067105

Faas, F.G., M.C. Avramut, B.M. van den Berg, A.M. Mommaas, A.J. Koster, and R.B. Ravelli. 2012. Virtual nanoscopy: generation of ultra-large high resolution electron microscopy maps. *J. Cell Biol.* 198:457–469. http://dx.doi.org/10.1083/jcb.201201140

Fidock, M., and B. DeSilva. 2012. Bioanalysis of biomarkers for drug development. *Bioanalysis*. 4:2425–2426. http://dx.doi.org/10.4155/bio.12.253

Fitch, C.D., G.Z. Cai, Y.F. Chen, and J.S. Ryerse. 2003. Relationship of chloroquine-induced redistribution of a neutral aminopeptidase to hemoglobin accumulation in malaria parasites. *Arch. Biochem. Biophys.* 410:296–306. http://dx.doi.org/10.1016/S0003-9861(02)00688-4

Goldberg, D.E. 2005. Hemoglobin degradation. *Curr. Top. Microbiol. Immunol.* 295:275–291.

Jani, D., R. Nagarkatti, W. Beatty, R. Angel, C. Slebodnick, J. Andersen, S. Kumar, and D. Rathore. 2008. HDP-a novel heme detoxification protein

Downloaded from jem.rupress.org on June 23, 2015

Published May 4, 2015

from the malaria parasite. *PLoS Pathog.* 4:e1000053. http://dx.doi.org/10.1371/journal.ppat.1000053

Janse, C.J., and A.P. Waters. 1995. Plasmodium berghei: the application of cultivation and purification techniques to molecular studies of malaria parasites. *Parasitol. Today (Regul. Ed.).* 11:138–143. http://dx.doi.org/10.1016/0169-4758(95)80133-2

Janse, C.J., J. Ramesar, and A.P. Waters. 2006. High-efficiency transfection and drug selection of genetically transformed blood stages of the rodent malaria parasite Plasmodium berghei. *Nat. Protoc.* 1:346–356. http://dx.doi.org/10.1038/nprot.2006.53

Jeffers, V. 2010. Shedding light on Plasmodium knowlesi food vacuoles. A thesis submitted to Combined Faculties for the Natural Sciences and for Mathematics of the Ruperto-Carola University of Heidelberg for the degree of Doctor of Natural Sciences.

Kinnamon, K.E., A.L. Ager, and R.W. Orchard. 1976. Plasmodium berghei: combining folic acid antagonists for potentiation against malaria infections in mice. *Exp. Parasitol.* 40:95–102. http://dx.doi.org/10.1016/0014-4894(76)90070-9

Klemba, M., I. Gluzman, and D.E. Goldberg. 2004. A Plasmodium falciparum dipeptidyl aminopeptidase I participates in vacuolar hemoglobin degradation. *J. Biol. Chem.* 279:43000–43007. http://dx.doi.org/10.1074/jbc.M408123200

Klonis, N., M.P. Crespo-Ortiz, I. Bottova, N. Abu-Bakar, S. Kenny, P.J. Rosenthal, and L. Tilley. 2011. Artemisinin activity against Plasmodium falciparum requires hemoglobin uptake and digestion. *Proc. Natl. Acad. Sci. USA.* 108:11405–11410. http://dx.doi.org/10.1073/pnas.1104063108

Lin, J.W., T. Annoura, M. Sajid, S. Chevalley-Maurel, J. Ramesar, O. Klop, B.M. Franke-Fayard, C.J. Janse, and S.M. Khan. 2011. A novel 'gene insertion/marker out' (GIMO) method for transgene expression and gene complementation in rodent malaria parasites. *PLoS ONE.* 6:e29289. http://dx.doi.org/10.1371/journal.pone.0029289

Liu, J., E.S. Istvan, I.Y. Gluzman, J. Gross, and D.E. Goldberg. 2006. Plasmodium falciparum ensures its amino acid supply with multiple acquisition pathways and redundant proteolytic enzyme systems. *Proc. Natl. Acad. Sci. USA.* 103:8840–8845. http://dx.doi.org/10.1073/pnas.0601876103

Na, B.K., Y.A. Bae, Y.G. Zo, Y. Choe, S.H. Kim, P.V. Desai, M.A. Avery, C.S. Craik, T.S. Kim, P.J. Rosenthal, and Y. Kong. 2010. Biochemical properties of a novel cysteine protease of Plasmodium vivax, vivapain-4. *PLoS Negl. Trop. Dis.* 4:e849. http://dx.doi.org/10.1371/journal.pntd.0000849

Platel, D.F., F. Mangou, and J. Tribouley-Duret. 1999. Role of glutathione in the detoxification of ferriprotoporphyrin IX in chloroquine resistant Plasmodium berghei. *Mol. Biochem. Parasitol.* 98:215–223. http://dx.doi.org/10.1016/S0166-6851(98)00170-4

Ponpuak, M., M. Klemba, M. Park, I.Y. Gluzman, G.K. Lamppa, and D.E. Goldberg. 2007. A role for falcilysin in transit peptide degradation in the Plasmodium falciparum apicoplast. *Mol. Microbiol.* 63:314–334. http://dx.doi.org/10.1111/j.1365-2958.2006.05443.x

Price, R.N., L. von Seidlein, N. Valecha, F. Nosten, J.K. Baird, and N.J. White. 2014. Global extent of chloroquine-resistant Plasmodium vivax: a systematic review and meta-analysis. *Lancet Infect. Dis.* 14:982–991. http://dx.doi.org/10.1016/S1473-3099(14)70855-2

Schwarzer, E., F. Turrini, and P. Arese. 1994. A luminescence method for the quantitative determination of phagocytosis of erythrocytes, of malaria-parasitized erythrocytes and of malarial pigment. *Br. J. Haematol.* 88:740–745. http://dx.doi.org/10.1111/j.1365-2141.1994.tb05112.x

Sijwali, P.S., J. Koo, N. Singh, and P.J. Rosenthal. 2006. Gene disruptions demonstrate independent roles for the four falcipain cysteine proteases of Plasmodium falciparum. *Mol. Biochem. Parasitol.* 150:96–106. http://dx.doi.org/10.1016/j.molbiopara.2006.06.013

Slomianny, C., G. Prensier, and P. Charet. 1985. Comparative ultrastructural study of the process of hemoglobin degradation by P. berghei (Vincke and Lips, 1948) as a function of the state of maturity of the host cell. *J. Protozool.* 32:1–5. http://dx.doi.org/10.1111/j.1550-7408.1985.tb03003.x

Spaccapelo, R., C.J. Janse, S. Caterbi, B. Franke-Fayard, J.A. Bonilla, L.M. Syphard, M. Di Cristina, T. Dottorini, A. Savarino, A. Cassone, et al. 2010. Plasmepsin 4-deficient Plasmodium berghei are virulence attenuated and induce protective immunity against experimental malaria. *Am. J. Pathol.* 176:205–217. http://dx.doi.org/10.2353/ajpath.2010.090504

Subramanian, S., M. Hardt, Y. Choe, R.K. Niles, E.B. Johansen, J. Legac, J. Gut, I.D. Kerr, C.S. Craik, and P.J. Rosenthal. 2009. Hemoglobin cleavage site-specificity of the Plasmodium falciparum cysteine proteases falcipain-2 and falcipain-3. *PLoS ONE.* 4:e5156. http://dx.doi.org/10.1371/journal.pone.0005156

Suwanarusk, R., B. Russell, M. Chavchich, F. Chalfein, E. Kenangalem, V. Kosaisavee, B. Prasetyorini, K.A. Piera, M. Barends, A. Brockman, et al. 2007. Chloroquine resistant Plasmodium vivax: in vitro characterisation and association with molecular polymorphisms. *PLoS ONE.* 2:e1089. http://dx.doi.org/10.1371/journal.pone.0001089

Vaid, A., R. Ranjan, W.A. Smythe, H.C. Hoppe, and P. Sharma. 2010. PfPI3K, a phosphatidylinositol-3 kinase from Plasmodium falciparum, is exported to the host erythrocyte and is involved in hemoglobin trafficking. *Blood.* 115:2500–2507. http://dx.doi.org/10.1182/blood-2009-08-238972

Downloaded from jem.rupress.org on June 23, 2015

Table S1. *P.berghei* Genes targeted in this study

Product name *P. falciparum* Gene ID	Localization (Pf)	Essential for blood stages (Pf)	Product name *P. berghei* Gene ID	Essential for blood stages (Pb) *	Product name *P. vivax* Gene ID
aspartic endoprotease					
plasmepsin I (PM I) PF3D7_1407900	DV	no	-	-	
plasmepsin II (PM II) PF3D7_1408000	DV	no	-	-	
plasmepsin IV (PM IV) PF3D7_1407800	DV	no	plasmepsin 4 (PM4) PBANKA_103440	no	plasmepsin 4 (PM4) PVX_086040
plasmepsin III (PM III) PF3D7_1408100	DV	no	-	-	
papain-like cysteine endoprotease					
falcipain 2a (FP 2a) PF3D7_1115700	DV	no	berghepain-2 (BP2) PBANKA_093240	no *	vivapain-2(VX2) PVX_091415
falcipain 2b (FP 2b) PF3D7_1115300	DV	no	-	-	
falcipain 3 (FP 3) PF3D7_1115400	DV	yes	-	-	vivapain-3 (VX3) PVX_091410 vivapain-4 (VX4) PVX_091405
metallopeptidase					
falcilysin (FLN) PF3D7_1360800	DV, mitochondrion, apicoplast	yes	bergheilysin (BLN) PBANKA_113700	yes *	PVX_115000
dipeptidyl aminopeptidase					
dipeptidyl aminopeptidase 1 (DPAP1) PF3D7_1116700	DV	yes	dipeptidyl aminopeptidase 1 (DPAP1) PBANKA_093130	no *	PVX_091465
aminopeptidases					
aminopeptidase P (APP) PF3D7_1454400	DV, cytosol	yes	aminopeptidase P (APP) PBANKA_131810	no *	PVX_117760
M1- family alanyl aminopeptidase (M1AAP) PF3D7_1311800	DV, nucleus	yes	M1- family alanyl aminopeptidase (AAP) PBANKA_141030	yes *	PVX_122425
M17-family leucyl aminopeptidase (M17LAP) PF3D7_1446200	DV, cytosol	yes	M17-family leucyl aminopeptidase (LAP) PBANKA_130990	no *	PVX_118180
M18-family aspartyl aminopeptidase (M18DAP) PF3D7_0932300	cytosol	no	M18-family aspartyl aminopeptidase (DAP) PBANKA_083310	no *	PVX_087090
heme detoxification protein					
heme detoxification protein (HDP) PF3D7_1446800	DV	yes	heme detoxification protein (HDP) PBANKA_131060	yes *	PVX_118155
papain-like cysteine proteases					
falcipain 1 (FP 1) PF3D7_1458000	Apical end of merozoites	no	berghepain 1 (BP1) PBANKA_132170	no *	PVX_117565
dipeptidyl aminopeptidases					
dipeptidyl aminopeptidase 2 (DPAP2) PF3D7_1247800	-	-	dipeptidyl aminopeptidase 2 (DPAP2) PBANKA_146070	no *	PVX_101280
dipeptidyl aminopeptidase 3 (DPAP3) PF3D7_0404700	-	yes	dipeptidyl aminopeptidase 3 (DPAP3) PBANKA_100240	no *	PVX_001005

*, the phenotype observed in this study.
-, no published data.